

# 3D Electromagnetic Frequency Domain Simulation of a Filter Choke with a Multilayer Foil Winding

Stefan Schoos, Oliver Schwanitz



**Abstract**—In this paper, an approach of an OHMIC loss prediction with a 3D electromagnetic (EM) simulation in frequency domain of a filter choke with a multilayer foil winding is presented. Detailed informations are given on the geometric setup, assumptions are made that specify the problem class and how the results are obtained by the software. Subsequently, the results of two leading 3D simulation suits are compared with the results of a 2D simulation and actual measurement data from the device. Concluding suggestions are made for similar problems. [Schoos]

## I. INTRODUCTION

PRECISE loss prediction plays a key role in designing modern power electronic devices where loss management and reduction is crucial for any downsizing effort. Inductors, as commonly used passive filter components, often have to carry the whole line current, when placed e.g. at the output of a power electronic circuit. Therefore any loss reduction in these components can have a significant implication on the overall efficiency of the device. However the loss calculation can be challenging as uncertainties arise e.g. due to non linear material behaviour, frequency dependencies and complex geometry. Hence this topic is still of high scientific interest, a variety of different approaches exist involving analytical formulas as well as numerical simulation. Despite the differences, the separation of inductor losses in winding and core losses is common ground. In order to achieve the desired inductor efficiency both loss proportions have to be carefully balanced. This requires precise knowledge of both core and OHMIC losses [1], [2].

This paper focusses on obtaining the OHMIC loss component of a multilayer foil winding choke with a 3D finite element method (FEM) electromagnetic simulation approach in frequency domain. The objective is to conduct comparable 3D FEM simulations of two leading commercial simulation suits, CST EM STUDIO 2014.01 from CST Simulation Technology AG [3] and MAXWELL 16.1 from ANSYS Inc. [4]. From the design phase of the choke are also results from the non commercial planar magnetics solver FEMM 4.2 [5], as well as measurement data from the actual prototype available. Those were gained with an precision impedance analyser 4294A from Agilent Technologies [6] and are provided with kind permission by the Fraunhofer IZM Berlin. Comparing the different simulation types to the measurement data, makes it possible to estimate the benefit of the 3D approach. As the 2D FEM solver cannot take the whole geometry into account, different results are expected from the 3D simulation. [Schoos]

## II. GEOMETRY OF THE FILTER CHOKE, MATERIAL- AND OPERATIONAL PARAMETERS

As it can be seen in FIG. 1, the winding is completely encapsulated by a surrounding ferrite housing to prevent exiting stray fields. The housing constitutes the yoke as well as the outer legs of the inductor and provides one part of the path for the magnetic flux. In the model, the magnetic material is assumed as linear, homogeneous, isotropic and time independent. The magnetomotive force is exerted at the inner leg around which the winding is placed. Due to the high permeability ( $\mu_r = 1000$ ) of the ferrite housing and core, a distributed air gap was required for the core, to achieve a required inductance of approximately  $7 \mu\text{H}$ . Additional losses by induced eddy currents are suppressed by using the distributed air gap.

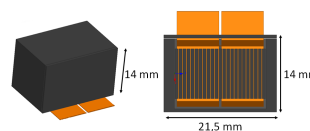


Fig. 1: Outer geometric setup of the choke

The winding of the filter choke consists of four layers of copper sheets, with a height of  $20 \mu\text{m}$ , a width of 8 mm and an conductivity of  $\sigma = 5,7 \cdot 10^6 \frac{\text{A}}{\text{Vm}}$ . The first winding is wound from the outside inwards, whereas the second winding is wound from the inside outwards. The reversal of the winding direction is realised by an orthogonal bending of the foil layers, as depicted in FIG. 2.

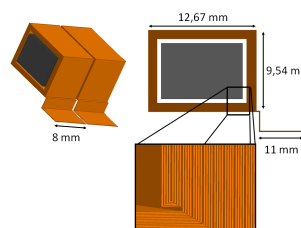


Fig. 2: Geometric setup of the winding

This is done to ensure the current distribution to be equally balanced by creating similar loop inductances for each layer. The maximum operational frequency of the filter choke is 5 MHz and the permittivity  $\epsilon = \epsilon_0$ . [Schoos, Schwanitz]

## III. CLASSIFICATION OF THE GIVEN PROBLEM IN THE ELECTROMAGNETIC THEORY

Before entering the theory of numerical analysis of the given structure, it is necessary to classify the problem in terms

of the electromagnetic theory. This means by looking at the geometric setup and the given parameters from SECTION II, it is possible to categorize it as a magneto quasistationary (MQS) problem. This offers the advantage, to reduce the full set of the MAXWELL equations. In [7] and [9] are several methods published to validate these classification.

One of them is to compare the absolute values of current density and the displacement current given by AMPERE's law.

$$\vec{\nabla} \times \vec{H}(\vec{r}) = \vec{J}(\vec{r}) + j\omega\vec{D}(\vec{r}) \quad (1)$$

If the displacement current is much smaller than the current density, than a MQS approach is valid and the displacement current can be neglected. Unfortunately,  $\vec{J}(\vec{r})$  and  $\vec{D}(\vec{r})$  are quantities which need to be determined by the simulation, but by using the following two linear relationships, the comparison only depends on already known parameters from SECTION II:

$$\vec{J}(\vec{r}) = \sigma\vec{E}(\vec{r}), \quad \vec{D}(\vec{r}) = \varepsilon\vec{E}(\vec{r}) \quad (2)$$

$$\left\| \vec{J}(\vec{r}) \right\| \gg \left\| \omega\vec{D}(\vec{r}) \right\| \iff \left\| \frac{1}{f} \right\| \gg \left\| \frac{\varepsilon}{\sigma} \right\|. \quad (3)$$

Thus, it is a comparison of the reciprocal maximum operational frequency and the relaxation time. However, the comparison is not useful for high conductivity given by the copper foil. Instead of the relaxation time, the average drift time of an electron in copper ( $T_r \approx 2.5 \cdot 10^{-14}$  s), should be used, [7] p.165.

$$\frac{1}{5} \cdot 10^{-6} \text{ s} \gg 2.5 \cdot 10^{-14} \text{ s} \quad (4)$$

It is obvious, that the left hand side is much bigger than the right hand side. The neglect of the displacement current in AMPERE's law for the simulation is thus possible. [Schwanitz]

$$\vec{D}(\vec{r}) = 0 \iff \vec{\nabla} \times \vec{H}(\vec{r}) = \vec{J}(\vec{r}) \quad (5)$$

#### IV. THEORY OF NUMERICAL SIMULATION

As written in section SECTION I, CST EM STUDIO, MAXWELL and FEMM are used to calculate the unknown quantities from SECTION I. All of them are using the FEM for an individual given partial differential equation (PDE) set with a specific calculation domain. In principle this calculation domain is discretized by a tetrahedral mesh with an amount of unknown nodes. CST EM STUDIO and FEMM are using a vectorized POISSON equation as their PDE to determine the magnetic vector potential  $\vec{A}$ , while Maxwell uses a HELMHOLTZ equation to determine the magnetic field  $\vec{H}$ . The unknown function from the PDE is in principle approximated by a sum of ansatz functions, each weighted with an unknown coefficient. These unknown coefficients are the given mesh nodes which need to be determined. All three programs are using NEDELEG WHITNEY edge functions as their ansatz functions. [Schwanitz]

#### A. Order of ansatz functions and adaptive mesh refinement

It is possible to vary the order of the ansatz functions to get additional nodes. A quadratic or cubic order, can bring much "better" results in comparison to a first order (standard) solution. Whereby "better" have to be clearly mathematical defined by an error definition. By using higher order ansatz functions, the computation time rises compared to a first order approach.

Another option is to change the adaptive mesh refinement. In principle this is a value in percent for a finer mesh generation in regions where actual solution could may be "false" or not "accurate" enough. A quantity which gives the informations if a solution could much more "accurate" ore "better", is the relative energy error. It is defined by a comparison of the whole energy in den calculation domain between the actual solution and the solution before. Is the difference between them less then a specific value, then a sign is given that the actual computed solution could be valid. [Schwanitz]

#### B. Boundary condition

All three simulation programs are using DIRICHLET boundary conditions applied to their calculation domains. Accordingly to the referred PDE's in the beginning of this section, CST EM STUDIO and FEMM are using the following formulation for the magnetic vector potential

$$\vec{n} \times \vec{A}(\vec{r}) = 0. \quad (6)$$

While MAXWELL uses a formulation for the magnetic field. [Schwanitz]

$$\vec{n} \cdot \vec{H}(\vec{r}) = 0 \quad (7)$$

#### C. Divergence check

Another important aspect for the EM simulation is to ensure that the divergence of current density  $\vec{J}(\vec{r})$  in the calculation domain is zero. The condition follows by taking the divergence of equation (5).

$$\vec{\nabla} \cdot (\vec{\nabla} \times \vec{H}(\vec{r})) = \vec{\nabla} \cdot \vec{J}(\vec{r}) \quad (8)$$

For topologically trivial domains, the following statement holds true.

$$\vec{\nabla} \cdot (\vec{\nabla} \times \vec{H}(\vec{r})) \equiv 0 \quad (9)$$

It follows that

$$\vec{\nabla} \cdot \vec{J}(\vec{r}) = 0. \quad (10)$$

This equation is characteristic for a MQS model [7] p.157, and have to be preserved in the numerical analysis, otherwise the given results could be false. [Schwanitz]

#### D. Calculation of the resistance and inductance

To calculate the resistance of the filter choke, it is necessary to know the OHMIC losses of the structure. For the given time harmonic electric field, which is determined by the FEM, the OHMIC losses can be determined by the following equation:

$$\overline{P}_v = \frac{\sigma}{2} \int_V |\vec{E}(\vec{r})|^2 dV. \quad (11)$$

Where  $\overline{P}_v$  are the time averaged OHMIC losses and  $V$  is the whole calculation domain.

By using also OHM'S law

$$\overline{P}_v = I_{\text{RMS}}^2 R, \quad (12)$$

for the losses, it is possible to determine the resistance of the filter choke.

$$R = \frac{\sigma}{2I_{\text{RMS}}^2} \int_V |\vec{E}(\vec{r})|^2 dV \quad (13)$$

By using the time averaged magnetic energy of the volume, with the known assumptions for  $\mu$  from SECTION II,

$$\overline{W}_m = \frac{\mu}{4} \int_V |\vec{H}(\vec{r})|^2 dV, \quad (14)$$

and the relationship for the inductance and magnetic energy.

$$\overline{W}_m = \frac{L}{2} I_{\text{RMS}}^2 \quad (15)$$

The inductance itself can then be calculated, using:

$$L = \frac{\mu}{2I_{\text{RMS}}^2} \int_V |\vec{H}(\vec{r})|^2 dV. \quad (16)$$

[Schwanitz]

## V. MODEL CREATION AND SIMULATION SETUP

In order to perform comparable simulation results, the model had to be identical in each of the 3D simulation suits. Therefore it was created in one program, afterwards exported and then reimported into the other. According to the problem classification, an MQS solver was used and the properties displayed in TABLE I were set in both programs alike. Because not all options were available the same way in both simulation environments, TABLE I represents the overlap.

	Anslys Maxwell	CST EM-Studio
Adaptive mesh refinement		10%
Min./Max. number of passes		2/10
Solver type		iterative
Relative energy error		1%

TABLE I: Solver properties

The boundary conditions were applied according to SECTION III. The boundary spacing is set to 10% of the maximum model edge size in each direction. This setting was chosen from experience with similar problems. In order to place the excitation terminals, the winding connections were extended to the model boundary and there short circuited to model possible effects due to imbalanced current distribution correctly. The shorting was accomplished using solid copper blocks which served as a model for the soldering attachment of the actual device. The outer face of these blocks was directly placed on the boundary and used for imprinting the excitation current. The excitation currents were set to  $1 A_{\text{RMS}}$  each. In FIG. 3 an overview of the simulation setup can be seen. [Schoos]

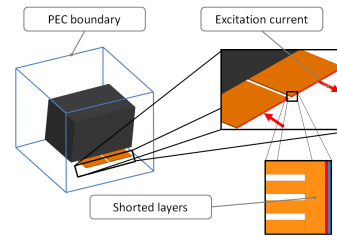


Fig. 3: Simulation setup

## VI. PROBLEMS WITH THE SIMULATION MODEL

The simulation suits showed individual error behaviour which made adoptions, in each program separate, necessary. CST EM STUDIO in particular showed several problems in creating the overall mesh. This was solved by creating a local meshing group with a finer discretization only for the air gap clearance. As just increasing the overall number of meshing cells led to no improvement, it seems that the algorithm failed to construct proper meshing cells at the junction from ferrite to air. With the local meshing group, a finer discretization is realized. But even with successful meshing, the CST EM STUDIO simulations kept failing. As the log file revealed, the simulations suffered from insufficient memory on the machine provided by the TU Berlin. After several tests, it was decided to drastically reduce the solver frequency range to  $f = 100 \text{ Hz} - 10 \text{ kHz}$  in order to extract at least limited results. MAXWELL runs on a cluster server at the Fraunhofer IZM enabling to overcome most of the hardware insufficiencies. Still the simulations showed poor convergence and long simulation times. Concluding, it can be stated that both simulation environments showed problems dealing with the multi scale geometry. [Schoos]

## VII. RESULTS

### A. Comparison of CST EM STUDIO and ANSYS Maxwell

As noted in SECTION VI only limited results from CST EM STUDIO were available due to hardware limitations. To yield comparable results the MAXWELL setup was reduced in the same way. The results are depicted in Fig. 4. In order to provide an orientation in terms magnitude, the results of FEMM, as well as extrapolated measurement data is also depicted. The latter is not intended for direct comparison as measurement was impossible below approximately 10 kHz due to a low signal to noise ratio. But an almost constant behaviour is expected in this frequency range, so the depicting is considered reasonable. As it can be seen in FIG. 4 the calculated inductances show opposite tendencies over the frequency sweep: rising in MAXWELL and dropping CST EM STUDIO.

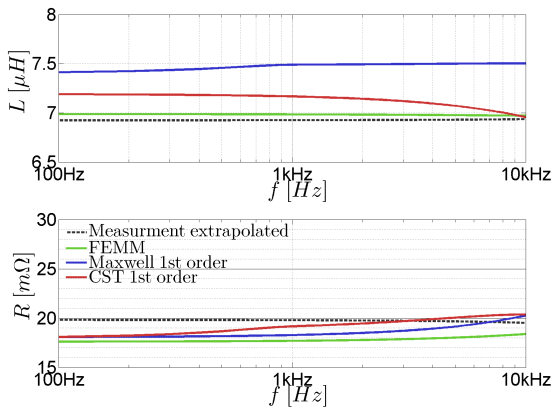


Fig. 4: Calculated inductance and resistance for the reduced setup (100 Hz to 10 kHz)

Both behaviours are unexpected, as the inductance should remain more or less constant at this frequency range or drop very slightly. The results of FEMM seem to be more reasonable at that point. This could be due to stability problems of the algorithms at low frequencies. The results for the more important factor in terms of loss prediction, the OHMIC resistance, seem to be more reasonable. At the low frequencies end they are almost the same as calculated with FEMM, ending up even closer to the first measured value. [Schoos]

### B. Evaluation of the 3D simulation

The previous comparison shows promising results for the computed OHMIC resistance, which made it desirable to compare the results over the whole frequency range. As mentioned in SECTION VI this was only possible on the cluster server at the Fraunhofer IZM, on which only MAXWELL was available. The results again show a clear deviation of the computed inductance with the 3D FEM approach compared to measurement data and the 2D simulation. But the overall tendency seems reasonable, showing the characteristic inductance drop, where the inner inductance decreases towards zero because of the skin and proximity effect. The shift by almost 10% could originate from small air gap deviations in the actual device to which the 2D FEM simulation, using effective values, then was adopted. The calculated inductance from the 3D simulation could represent the ideal case. The sharp rise of the inductance in the plot of the measurement data, at 1 MHz shows the first resonance with the winding capacitance. As the displacement current is neglected in the MQS approach, this is not visible in the plot of the simulations. Below that frequency, the measurement error should be significantly below 10% according to the manual of the impedance analyzer [8], so it can be used for a comparison. Until 500 kHz, the measured OHMIC resistance and computed values are almost congruent. The loss prediction can be seen as accurate until that point. Surprisingly, the resistance shows a distinct frequency dependence, though the skin depth should be greater than the conductor height. This might be explained by the fact, that the commonly used formula for calculating the skin depth is only valid for conductors with large bending

radii. For the used foil sheets with sharp edges, an increased resistance is clearly visible. [Schoos]

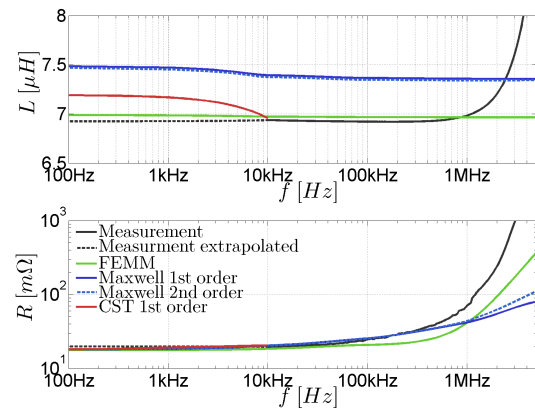


Fig. 5: Calculated inductance and resistance from 100 Hz to 5 MHz with ANSYS Maxwell

### C. Examination of the benefit of higher order basis functions

From FIG. 5 it is visible, that the results from the first and second order basis function simulation only deviate little at the end of the frequency range. Therefore, it is not desirable to use higher order basis functions. [Schoos]

## VIII. CONCLUSION

In this paper, a 3D FEM simulation of a filter choke was discussed. It was shown that the obtained simulation results are in the same order of magnitude like the measurement data. The comparison between the 2D and the 3D simulation clearly revealed, that even at complex geometry 2D simulation can have advantage over a 3D simulation. 2D simulation might therefore be more valuable for an engineer in the design phase of a component. For accurate loss prediction and the evaluation of the final design, a 3D simulation proves to be the more valuable tool for further investigation of optimization options. Yet the 3D simulation leads to significantly higher requirements in time and computing power. As a starting point, the standard first order basis functions proved to be the most efficient and robust way to perform the presented simulation scenario. [Schoos]

## REFERENCES

- [1] S.Hoffmann, Prof.-Dr. E.Hoene, "Reducing Inductor Size in High Frequency Grid Feeding Inverters," PCIM Europe 2015, Special Session on Passive Components
- [2] W.G. Hurley, W.H. Wölflle, "Transformers and Inductors for Power Electronics - Theory Design and Applications," 2013 John Wiley & Son Ltd.
- [3] CST Computer Simulation Technology AG, www.cst.com
- [4] ANSYS Inc., www.ansys.com
- [5] David Meeker, FEMM 4.2, www.femm.info
- [6] Agilent Technologies, www.agilent.com
- [7] H.Henke, "Elektromagnetische Felder - Theorie und Anwendung," 4. edited edition, 2011, Springer Heidelberg Dordrecht London New York
- [8] Agilent Technologies, "Agilent 4294A Precision Impedance Analyzer Operation Manual," 7. edition, 2003, Agilent Technologies
- [9] G.Benderskaya, "Numerical Methods for Transient Field-Circuit Coupled Simulations Based on the Finite Integration Technique and a Mixed Circuit Formulation, 2007, TU- Darmstadt